Benítez-González, J.; Bolea Boluda, M.; Mora Almerich, J. (2017). High performance low coherence interferometry using SSB modulation. IEEE Photonics Technology Letters. 29(1):90-93. doi:10.1109/LPT.2016.2628963

High performance low coherence interferometry using SSB modulation

J. Benítez, M. Bolea, J. Mora

***Abstract*— Low coherence interferometry (LCI) is an optical measurement technique that has attracted the interest for relevant fields like medicine or sensing. With the objective of improving LCI capabilities, microwave photonics (MWP) arises as an innovative technology to enhance LCI possibilities. In this work, a novel MWP-LCI approach is proposed and experimentally demonstrated to measure the optical path difference (OPD) of a sample. The operation principle of the technique is based on the analysis of the interference pattern through a dispersive element to retrieve its visibility using a vector network analyzer. Different capabilities of the system in terms of sensitivity, resolution and SNR have been proved. In this case, the proposal is able to avoid carrier-suppression-effect leading to a sensitivity improvement of 20 dB in comparison with previous structures for certain values of the OPD. Moreover, the OPD range has been extended up to 10 mm achieving an invariant resolution over all operation range. Finally, the improvement of the SNR of the system has been experimentally demonstrated by controlling properly the RF resonance profile through the adjustment of the optical source power distribution. We have observed an improvement of the dynamic range close to 40 dB for a Gaussian profile.**

***Index Terms*— Microwave Photonics, Low Coherence Interferometry, Optical Path Delay, Dispersive element, Single-Sideband Modulation**

I. Introduction

Low coherence interferometry (LCI) constitutes a widespread optical technique for high-resolution axial positioning measurement. For the last decades, LCI has been dramatically extended to a huge number of application fields such as: optical components characterization [1], art conservation [2], medical diagnosis [3-5] and sensing [6]. Nevertheless, optical coherence tomography (OCT) can be considered the main responsible of the great development of LCI. Indeed, OCT has become a powerful technique for medical diagnosis. According to the interest in OCT applications, current LCI research focuses on the improvement of key performance parameters, specifically in terms of stability, resolution, sensitivity and scanning speed, in most cases limited to a single interferometric structure [4].

The operation principle of LCI is based on the measurement of the echo time delay of backscattered light in a sample through the characterization of the interference intensity obtained when the light coming from the sample and the light reflected in a reference surface overlap. When a low coherence source is used, the interference signal is temporally and spatially localized, so it is possible the use of this property to obtain the optical path difference (OPD) of interfering beams and to determine the values of the physical quantities which give rise to the measured OPD. This fact, together with the use of continuous-wave low-coherence or broadband sources (BBS), offers spatial resolutions of microns [7].

Although specifications suitable for current LCI solutions can be found, the stability is a drawback since its improvement increases the system complexity with an extra built cost. In this context, microwave photonics (MWP) can offer significant benefits to LCI systems due to the inherent stability of the interference pattern in the radio-frequency (RF) domain under environmental variations without compromising overall LCI performance. As known, MWP is defined as the study of photonic devices operating at microwave frequencies and their applications to microwave and optical systems [8]. Although MWP development over the past 30 years runs in parallel with the field of communications, MWP has been also introduced in photonic emerging applications such as MWP-filtering for sensor interrogation, terahertz-wave generation and processing for non-invasive high-resolution sensing and MWP-based quantum key distribution are potential applications [9].

The establishment of a correspondence between LCI and MWP systems opens a new way to comparatively explore the adaptation of MWP structures from a LCI perspective leading to MWP-LCI technology. In this sense, recently, it has been proposed a method for retrieving the visibility of low-coherence interferograms based on the use of a single-bandpass MWP filter [10]. Nevertheless, the range of the OPD is limited to 5 mm due to the carrier suppression effect (CSE), responsible of the RF fading of double sideband (DSB) modulated optical signals in dispersive media. Moreover, axial resolution is decreased for penetration distances further than 1.5 mm as a consequence of the third order dispersion effects.

In this letter, we propose the adaptation of a microwave photonic structure for LCI measurements based on the slicing

Manuscript received August 1st, 2016. The research leading to these results has received funding from the National Project TEC2014-60378-C2-1-R funded by the Ministerio de Ciencia y Tecnología and the regional project PROMETEO FASE II/2013/012 funded by the Generalitat Valenciana.

J Benítez, M. Bolea and J. Mora are with the ITEAM Research Institute, Universitat Politècnica de València, Valencia, Spain (e-mail: jmalmer@iteam.upv.es).

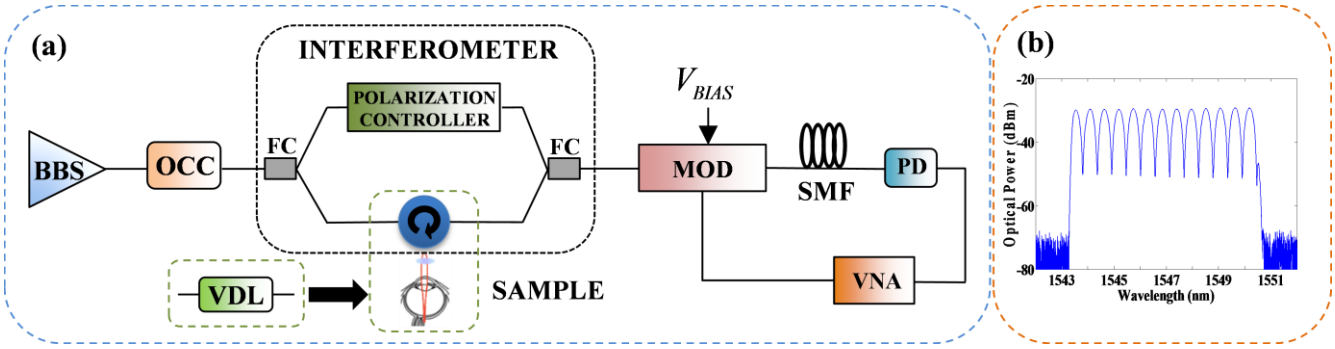

Fig. 1. (a) Proposed MWP-LCI structure. (b) Uniform optical source power profile for an OPD = 5.76 mm.

of a single sideband (SSB) modulated broadband source (BBS) and the analysis through a dispersive element. Compared to [10], LCI key parameters have been significantly improved. For instance, our proposal permits to increase the OPD range from 6 to 10 mm. Besides, the sensitivity and resolution remain constant in the complete OPD range since the CSE is avoided and the non-desired dispersive effects are controlled in our approach. In fact, an improvement of sensitivity more than 20 dB is achieved in comparison to [10]. Finally, we have also experimentally demonstrated the capability of the system for controlling the RF resonance profile improving both signal to noise ratio (SNR) and sensitivity range.

II. System Description

Fig. 1 shows the MWP-LCI structure based on a microwave single-passband filter [12] employing SSB modulation [13]. An incoherent optical source is considered to be launched into an inteferometric structure which leads to retrieve the OPD of a sample through the interference pattern. The output signal after the interferometer structure is described as:

$$T(\omega)=\frac{1}{2}S(\omega)\cdot\left[1+V\cdot cos\left(\frac{2n\omega}{c}OPD+\xi\right)\right] \quad (1)$$

where $S(\omega)$ is the optical power spectral density, V is the visibility of the interference, n is the refraction index of the interferometer's arms, c is the light speed in vacuum and ξ is the phase drift of the interferometer.

In the experimental scheme, the optical signal is provided by the combination of a Broadband Source (BBS), with a total optical bandwidth of 80 nm, and an Optical Channel Controller (OCC), which allows generating the optical power profile desired. The OCC is centered at 1546.92 nm and has 48 channels of 0.8 nm each, which attenuation can be independently controlled.

The interferometric structure is based on a Mach-Zehnder Interferometer (MZI). One of the arms of the interferometer is composed by a polarization controller device, which ensures the maximum visibility of the interference pattern. In order to experimentally evaluate the system performance, a variable delay line (VDL) has been placed in the arm under test which allows tuning the OPD under test. For instance, the OCC is set to obtain a uniform optical source power profile with 7.2 nm of bandwidth. Fig. 1(b) shows the optical spectrum after the interferometric structure generating a slicing pattern directly related to the Optical Path Difference (OPD) of the sample. In this case, an OPD of 5.76 mm is considered.

In addition, the MWP-LCI system performs an RF modulation process (MOD) after the interferometric structure. In this case, a single sideband (SSB) modulation is considered as key difference compared to previous works based on amplitude modulation [10]. The SSB modulation is considered by means of a dual drive modulator (Sumitomo Osaka Cement 33 GHz) in combination with a 90º Hybrid Coupler [11]. The SSB modulator is driven by a single RF tone Ω which leads to obtain the RF transfer function by means of a vector network analyzer (VNA). Note that phase information is not needed in our system. Therefore the built cost could be considerably reduced by introducing a tunable oscillator as replacement for the VNA.

After the optical signal modulation, a standard single mode fiber (SMF) is considered as dispersive element, which main properties are the length (L) and the dispersion parameter, β_2 = -22 ps^2/km. Finally, the optical signal is photodetected (PD) (u2t BPDV2020R-VF-FP). The system performance is evaluated by means of the transfer function, which has been recorded in the frequency range of 10 MHz – 25 GHz by means of a VNA (Agilent E8364A).

In order to experimentally describe the performance of the proposed MWP-LCI scheme, Fig. 2 shows the electrical transfer functions when SSB is performed (blue line). To establish a proper comparison with previous works using amplitude modulation, a DSB intensity modulator (Photline

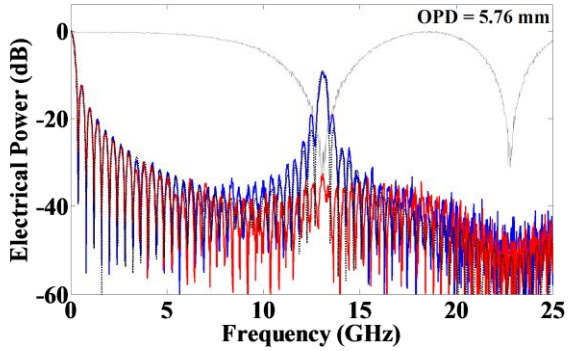

Fig. 2. Electrical transfer function obtained by the VNA when SSB modulation (blue line) and DSB modulation (red line) are performed. Theoretical simulation has been added in black dashed line. Besides, CSE for 20 km has been plotted in grey continuous line.

MZ6-0623) has been also used to obtain the corresponding experimental measurement. The DSB-RF transfer function is plotted in red line.

Firstly, we can observe in Fig. 2 that the electrical transfer function for SSB modulation gives an RF resonance around 13.1 GHz related to the OPD of the device under test (DUT) set to 5.76 mm. This relationship between central frequency Ω_o and the corresponding OPD is according to the following expression similar to previous DSB schemes:

$$\Omega_o = -\frac{2 \cdot OPD}{c_0 \beta_2 L} \quad (2)$$

where β_2 and L refer to the dispersion and effective length of the dispersive element, respectively. In this case, a 20 km SMF link is considered as dispersive element with an accumulated dispersion of -440 ps^2 (β_2L).

In this way, the OPD measurement can be obtained through the electrical transfer function considering the proposal as an RF end-to-end system. In this case, the RF transfer function for this case can be written as [12]:

$$H_{SSB}(\Omega) \propto V \cdot S(\omega) \int S(\omega) \cdot e^{j\beta_2 L(\omega-\omega_o)(\Omega-\Omega_o)} d\omega \quad (3)$$

From Eq. (3), we observe that the carrier suppression effect (CSE) is avoided. When DSB modulation is considered, the sensitivity is critically affected by CSE due to the dispersion $\beta_2 L$ [10]. An RF fading appears according to the relationship $\cos(\beta_2 L \Omega^2/2)$ as shown in Fig. 2 (grey line). Therefore, our MWP-LCI proposal overcomes this limitation related DSB-modulated optical signals in dispersive media.

As can be observed in Fig. 2, the RF resonance is removed for an OPD of 5.76 mm when the DSB modulation is considered (red line). In this case, the first resonance of the CSE is located around 13.1 GHz which limits the system operation range up to few millimetres for DSB modulation [10]. By contrast, our SSB approach is free from CSE which allows overcoming this limitation and measure values of OPD higher than DSB schemes. This fact leads to an improvement of the signal to noise ratio in the complete OPD range considered. Note that Fig. 2 includes the theoretical RF transfer function for SSB configuration and demonstrates an excellent agreement with the experimental measurement.

III. Experimental Results

In this section, different capabilities of the MWP-LCI structure proposed are experimentally demonstrated. Particularly, in terms of sensitivity, relationship of the RF resonance central frequency with the OPD, resolution and Signal-to-Noise (SNR) ratio, which suppose the most representative parameters of the scheme proposed and for LCI techniques. The electrical transfer function of the system for different OPD values has been measured to obtain and analyze the RF resonances generated.

Firstly, the RF resonance central frequency has been measured with its corresponding OPD value in order to show the relation between both magnitudes. Experimental results obtained for SSB (•) are depicted in Fig. 3. The frequency range measured is 0-25 GHz, leading to a maximum OPD value of 10 mm. An excellent linear behaviour between central frequency and OPD can be observed, with a slope around 2.30 GHz/mm as predicted in Eq. (2). In this way, our approach permits the OPD measurement through the central frequency of the RF transfer function shown in Eq. (2). In Fig. 3, experimental results obtained for DSB (■) are also plotted where the OPD is limited to 5.2 mm due to the first notch of the CSE located at the RF frequency 13.1 GHz [10].

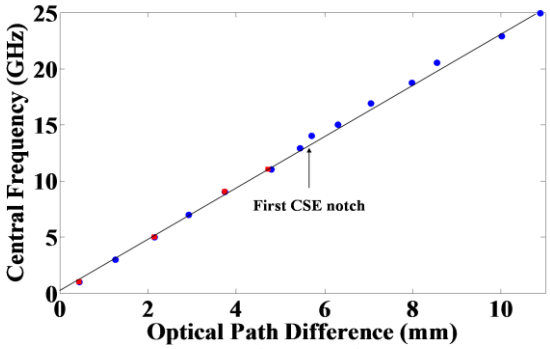

Fig. 3. RF resonance central frequency for SSB (•) and DSB (■) modulation versus OPD.

In the following, both modulation formats (SSB and DSB) have been considered to compare them in terms of sensitivity. As can be observed in Fig. 4, sensitivity is increasing with the frequency for both modulation formats in the 0–10 GHz range. This fact is due to the sensitivity is affected by the baseband component for low OPD values as shown in Fig. 2. Then, SSB and DSB modulation schemes achieve a maximum sensitivity higher than 35 dB. However, when the DSB modulation is performed (■) sensitivity drops to levels below 20 dB when the CSE notches appear, i.e., for 13.1 GHz. Therefore, the useful OPD range is restricted since for certain OPD values the interference pattern is not consistent. In contrast, when the SSB format is employed (•), our approach permits a constant sensitivity in all the OPD range since the CSE is avoided. In this case, sensitivity levels achieved are over 35 dB, leading to an improvement further than 20 dB respected to previous DSB cases [10].

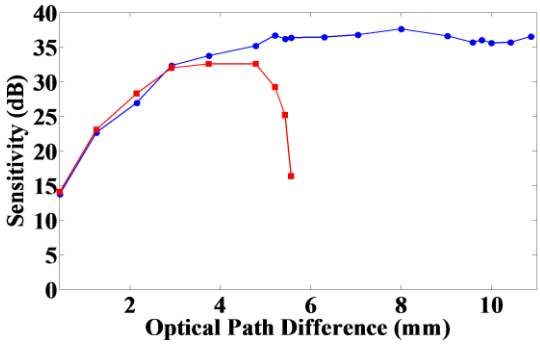

Fig. 4. Sensitivity of the system for SSB (•) and DSB (■) modulation versus OPD.

Furthermore, resolution is one of the most important LCI parameters as it describes the maximum precision that the system is able to reach in order to obtain the sample information. For this case, experimental results to address the resolution of the MWP-LCI structure proposed have been

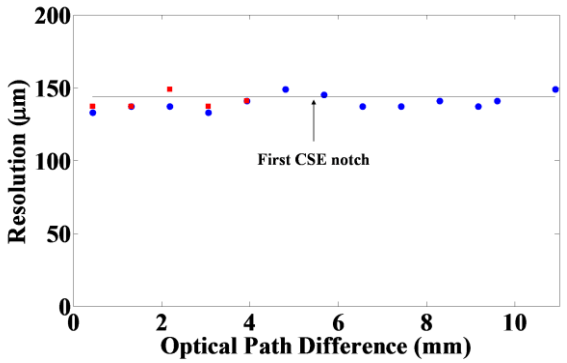

Fig. 5. Resolution versus OPD for SSB (•) and DSB (■) modulation.

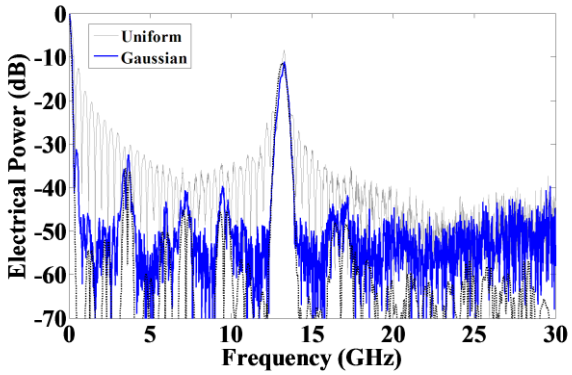

Fig. 6. Electrical transfer functions of the RF resonance when a uniform profile (grey line) and a Gaussian profile (blue line) are employed in the optical source. Theoretical simulation of gaussian profile in black dashed line.

estimated. In conventional LCI techniques, the axial resolution (δz) is proportional to $\lambda^2/\Delta\lambda$ where Δλ is the optical source bandwidth and λ corresponds to the central operation wavelength of the optical source. Attending to MWP-LCI point of view, resolution relates the electrical bandwidth of the resonance and the main parameters of the dispersive element: $\delta z = c_0 \cdot \pi \cdot |\beta_2 \cdot L| \cdot BW_{elec}$. According to this definition, the electrical bandwidth of the RF resonance for different OPDs has been measured. Resolution experimental results have been depicted in Fig 5 for SSB and DSB schemes. As can be observed, the resolution is maintained practically constant for both configurations close to the theoretical value of 147 μm (black line). Note that resolution is not defined for certain values of the OPD when DSB is considered, since the RF resonance is removed due the CSE. Additionally, when SSB modulation is used, the resolution is maintained in the whole OPD range since the third-order dispersion coefficient is not relevant [10].

Finally, we show the improvement of the dynamic range by employing an apodization on the optical source power profile. Fig. 6 shows the electrical transfer function when a Gaussian profile is employed with a 3-dB optical bandwidth of 7.2 nm and the uniform profile corresponding to Fig. 1(b). As observed, the secondary sidelobes of the baseband contribution are reduced up to 40 dB for the Gaussian profile. Therefore, the dynamic range is considerably increased respect to the uniform profile with an improvement of the sensitivity for low OPD values. Moreover, the theoretical simulation for the Gaussian profile has been included (black dashed line of Fig. 6) in order to show a good agreement with the experimental result.

IV. Conclusions

A novel MWP-LCI approach has been proposed in order to enhance LCI parameters. The key difference from previous schemes lies in the use of a different modulation format from DSB to SSB. To establish a suitable comparison, SSB and DSB modulation formats have been implemented by the use of a dual-drive modulator. Our approach permits to overcome the limitations related to the CSE when DSB is considered. Indeed, when SSB modulation is performed, CSE is avoided leading to an improvement in terms of OPD range measurement and sensitivity in comparison to DSB structures. A linear behaviour between the OPD and the central frequency of the RF resonance has been experimentally demonstrated. In this sense, we achieve a maximum OPD close to 10 mm which is significantly more than previous schemes. Besides, the system resolution is practically constant in all the OPD. Finally, we improve considerably the dynamic range of the system by controlling the power spectral density of the optical source since the electrical transfer function can be apodized.

References

[1] C. Y. Chen, C. Y. Wang and Y. J. Chen, "Analysis of SOI micro ring resonator with reflection property using low coherence interferometry method," in *OECC/ACOFT 2014*, Melbourne, Australia, July 2014, pp. 260-262.

[2] P. Targowski and M. Iwanicka, "Optical Coherence Tomography: its role in the non-invasive structural examination and conservation of cultural heritage objects - a review," *Appl. Phys. A*, vol. 106, no. 2, pp. 265-277, Feb. 2012.

[3] D Huang, E. A. Swanson, C. P. Lin, J. S. Schuman, W. G. Stinson, W. Chang, M. R. Hee, T. Flotte, K. Gregory, C. A. Puliafito, "Optical Coherence Tomography," *Science*, vol. 254, pp. 1178-1181, Nov. 1991.

[4] A. Gh. Podoleanu, "Optical Coherence Tomography," *J. of Microscopy*, vol. 247, no. 3, pp. 209-219, Sep. 2012.

[5] W. Drexler and J. G. Fujimoto, "State-of-art retinal optical coherence tomography," *Progress in Retinal and Eye Research*, vol. 27, no 1, pp. 45-88, Jan. 2008.

[6] Y.-J. Rao and D. A Jackson, "Recent progress in fibre optic low-coherence interferometry," *Meas. Sci. Technol.*, vol. 7, pp. 981-999, Jul. 1996.

[7] A. F. Fercher, W. Drexler, C. K. Hitzenberger and T. Lasser, "Optical coherence tomography - principles and applications," *Rep. Prog. Phys.*, vol. 66, pp. 239-303, Jan. 2003.

[8] J. Capmany and D. Novak, "Microwave Photonics combines two worlds," *Nat. Photonics*, vol. 1, pp. 319-329, Jun. 2007.

[9] J. Capmany, J. Mora, I. Gasulla, J. Sancho, J. Lloret, S. Sales. "Microwave Photonics signal processing," *J. of Lightwave Tech.*, vol. 21, no. 4, pp. 571-586, Oct. 2013.

[10] C. R. Fernandez-Pousa, J. Mora, H. Maestre, P. Corral, "Radio-frequency low-coherence interferometry," *Opt. Lett.*, vol. 39, no. 12, pp. 3634-3637, Jun. 2014.

[11] P. S. Devgan, D. P. Brown and R. L. Nelson, "RF Performance of Single Sideband Modulation Versus Dual Sideband Modulation in a Photonic Link," *J of Lightwave Tech.*, vol. 33, pp. 1888-1895, May 2015.

[12] J. Mora, B. Ortega, A. Díez, J. L. Cruz, M. V. Andrés, J. Capmany, and D. Pastor, "Photonic Microwave Tunable Single-Bandpass Filter Based on a Mach-Zehnder Interferometer," *J of Lightwave Tech.* 24, 2500-2509, 2006.

[13] G. H. Smith, D. Novak and Z. Ahmed, "Overcoming chromatic-dispersion effects in fiber-wireless systems incorporating external modulators," in *IEEE Trans. Microw. Theory Techn.*, vol. 45, no. 8, pp. 1410-1415, Aug 1997.